

VRBA2024-00001

ABRASIVE SURFACE TREATMENT OF AISI10MG PARTS MADE BY L-PBF

A. Mechali^{1*}, J. Mesicek¹, Q. -P Ma¹, J. Hajnys¹, P. Gautam¹, R. Blaha¹, D. Krisak¹, J. Petru¹

¹VSB -Technical University of Ostrava, Department of Machining Assembly and Engineering Metrology, Faculty of Mechanical Engineering, Ostrava, Czech Republic

*Abdesselam Mechali; e-mail: abdesselam.mechali.st@vsb

Abstract

The scientific community has been intensively studying how to improve the level of surface roughness on 3D-printed parts, particularly metallic parts made using the selective laser melting (SLM) technique. Various research papers on this subject have revealed that accurate surface roughness data can be generated using several methods that are, in fact, not cost-effective. For this reason, the finishing processes are an integral part of the overall production, especially for those components where the primary concern is not only appearance but also functional properties (e.g., lower friction, reduced noise, etc.). This work deals with the measurement of the surface roughness of tumbled parts produced with SLM after surface treatment with centrifugal and vibratory methods. Tumbling was performed with ceramic, plastic, and porcelain mediums. At the end, there is an evaluation of the measurement data based on the required surface roughness of the components.

Keywords:

Selective laser melting (SLM), surface roughness, abrasive surface finishing, AISI10Mg

1 INTRODUCTION

Designers may now create practical, lighter, and much more complicated pieces out of a range of materials thanks to 3D printing technology [Xiao 2018, Marsalek 2020]. Surprisingly, metal components made using selective laser melting (SLM) had greater mechanical qualities than ones made using more conventional methods [Pagac 2018, Liverani 2017]. The aerospace, healthcare, and automotive sectors, for example, employ a number of common alloys, and SLM technology has been developed to operate with them [Yakout 201, Chen 2018; Mohammadian 2018]. However, as discussed in [Strano 2013, Wang 2016, Leary 2017, Vayssette 2018].

The largest and most glaring flaw with 3D-printed items in general and SLM components in particular is the considerable surface roughness that arises from the printing process. The build chamber's position and direction, the inert gas stream's direction and flow rate, the powder's properties, and the power and laser velocity all have a substantial influence on the SLM products' surface roughness [Townsend 2016, Hajnys 2020, Kozior 2020].

The conventional computer numerical control (CNC) machining procedure must then be applied to SLM components in order to produce the necessary surface roughness, as was previously stated [Kaynak 2018, Cep 2014, Cillikova 2022].

In this scientific article, samples of stainless steel were created using AISI10Mg powder by employing the SLM

process for printing the samples, and these printed samples were then tumbled in three dissimilar mediums, respectively, ceramic, plastic, and porcelain, using two types of tumbling: centrifugal and vibratory tumbling. The results of each group of samples were investigated and then compared in order to acquire the printed samples with the least level of surface roughness. The challenge is to determine which finishing method will produce the highest-quality surface textures. Based on the measurement, an evaluation of the roughness of individual surfaces for future machining of additively manufactured components made of AISI10Mg material was performed. The work was carried out according to Figure 1, which illustrates the sequence of the experiment.

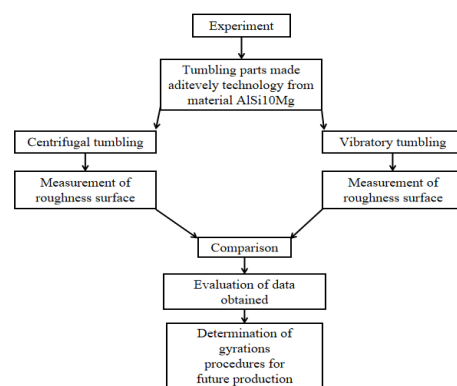


Fig. 1: Workflow of the experiment

2 MATERIAL AND

2.1 Powder characteristics

AlSi10Mg is an alloy composed mostly of silicon, aluminum, and relatively small amounts of magnesium, as shown in Table 1 after using scanning electron microscopy (SEM) on a JSM-6510 device (JEOL, Akishima, Japan), energy-dispersive spectroscopy (EDS), and Oxygen/Nitrogen/Hydrogen analyzer (ELTRA ONH 2000). The inclusion of silicon makes the alloy more durable and robust than aluminum alone with the Mg₂Si compound [Mesicek 2022]. The aluminum alloy has a thick oxide layer that forms naturally on its surface, providing it with excellent levels of corrosion resistance. This resistance can be increased even more by chemical anodizing [Bin 2018].

Tab. 1 : Chemical composition of the AlSi10Mg (at.%) [Mesicek 2022].

Component	EDS area analysis	ELTRA ONH 2000
O	4.7 +0.2	0.09 + 0.01
Mg	11.0 + 0.1	N/A
AL	84.1 + 0.2	N/A
Si	10.3 + 0.1	N/A

2.2 Morphology of the powder

The scanning electron microscopy (SEM) image of the AlSi10Mg powder is shown in Figure 2. The particles have a spherical form that is characteristic of powders formed as a result of gas atomization. This spherical shape causes roughness after scanning in the SLM printer due to the melting of the particles on the surface of the printed samples, as shown in Figure 3. It was noticed that there were numerous satellites (smaller particles adhering to bigger particle surfaces, which can size up to 10 µm). Most of the particles are 45 µm in size, and they follow a regular distribution with high flowability [Mesicek 2022].

Figure 3 presents a 3D surface roughness image taken for an as-built sample after 3D printing using an optical microscope called the Alicona InfiniteFocus 5G (IF MeasureSuite, Alicona ImagingGmbH, Raaba/Graz, Austria), which reveals that the sample's surface has peaks that are measured up to 0.18 mm.

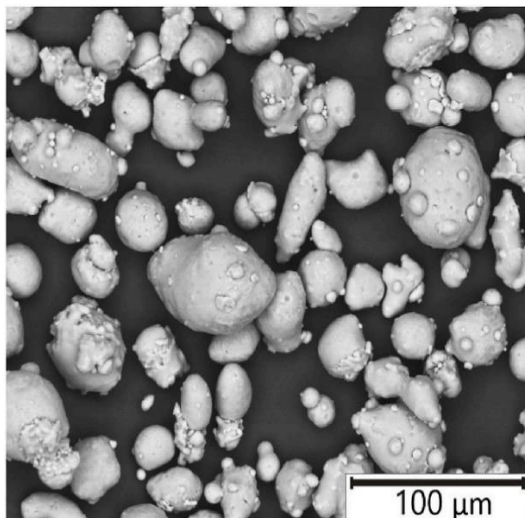


Fig. 2: SEM/BSE images showing the particle shapes of the AlSi10Mg powder. [Msicek 2022]

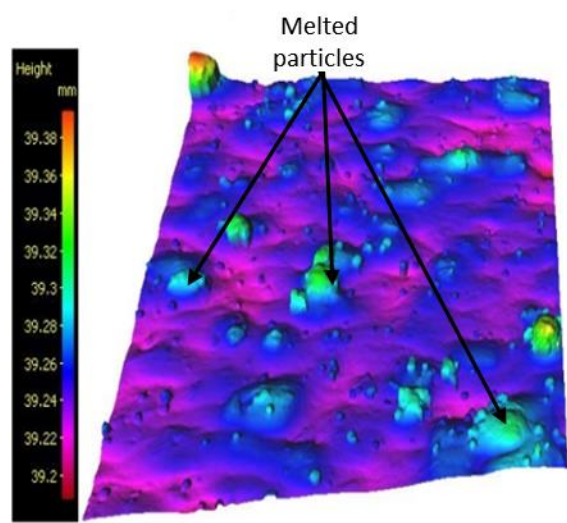


Fig. 3: 3D Surface structure of the as-built sample after 3D printing

2.3 3D Printing and printing parameter

A SLM Renishaw AM500 3D printer (Wotton-under-Edge, UK) with a laser with a highest rated power of 500 W was used to fabricate the samples. The inert gas was argon with a purity of 5.0, and the focus size was set to 70 µm. Air was driven out of the chamber and kept below 1000 ppm throughout the printing process to prevent the powder from oxidizing during setup and because the inert gas was inefficient at removing metal vapors during printing. The system was configured using QuantAM software (5.0.0.135, Renishaw, Wotton under Edge, UK). While printing the samples directly onto the substrate, no support materials were employed. To make samples with and without preheating the substrate, twenty samples were divided into two builds. The samples were numbered from 1 to 20, as shown in Figure 4. Printing on the bridge samples began with the pylons and progressed to the upper section.



Fig. 4: AlSi10Mg samples material after printing

2.4 2D and 3D surface roughness measurement

Following manufacturing, samples from 2 to 10 were centrifugally tumbled using the tumbler OTEC CF1 32EL. The machine was programmed to rotate 180 rpm. Subsequently, samples 12 to 20 were put through vibration tumbling cycles using a 60-liter container called an Avalon WR60. The set speed of the device was 1950 rpm. Tumbling was in three different mediums: ceramic (DZS 10/10, Otec company, Pforzheim, Germany), plastic (XS 12K, Wather Trowal company, Germany), and porcelain (P 2/5, Otec company). Samples 1 and 11 were as-built samples; samples 2, 3, 4, 12, 13, and 14 were tumbled in one tumbling cycle for 60 minutes in each type of tumbling medium. Samples 5 and 15 were tumbled for 60 minutes in all types of tumbling medium. Samples 6, 7, 8, 16, 17, and 18 underwent almost the same tumbling procedure, with the difference that for samples 6 and 16, there was one additional tumbling cycle in ceramic medium, for samples 7 and 17, one additional cycle in plastic medium, and for samples 8 and 18, one additional cycle in porcelain medium. Samples 9 and 19 passed tumbling for 120 minutes in a ceramic medium, 120 minutes in a plastic medium, and 60 minutes in a porcelain medium. The last samples (10 and 20) underwent two cycles in all tumbling mediums. Table 2 summarizes the matrix of tumbling methods and treatment times.

Subsequently, Mitutoyo SJ-210 was utilized to determine the 2D roughness of the surface as shown in Figure 5.(a). Every sample surface has been measured six times. In order to reduce the error of measurement, the arithmetical mean height of a line (R_a) and the mean roughness depth (R_z) were determined.

Eventually, 3D surface structure roughness was measured using the optical microscope Alicona InfiniteFocus 5G (IF MeasureSuite, Alicona ImagingGmbH, Raaba/Graz, Austria) as shown in Figure 5.(b).

Tab. 2: Matrix of tumbling methods and treatment time

Sample NO.	Tumbling method		Medium						Total time
			Ceramic		Plastic		Porcelain		
	Centrifugal	Vibratory	[min]	[min]	[min]	[min]	[min]	[min]	
1									0
2	X			X					60
3	X				X				60
4	X					X			60
5	X		X		X		X		180
6	X			X	X		X		240
7	X		X			X	X		240
8	X		X		X			X	300
9	X			X		X	X		300
10	X			X		X		X	360
11									0
12		X	X						60
13		X			X				60
14		X				X			60
15		X	X		X		X		180
16		X		X	X		X		240
17		X	X			X	X		240
18		X	X		X			X	300
19		X		X		X	X		300
20		X		X		X		X	360

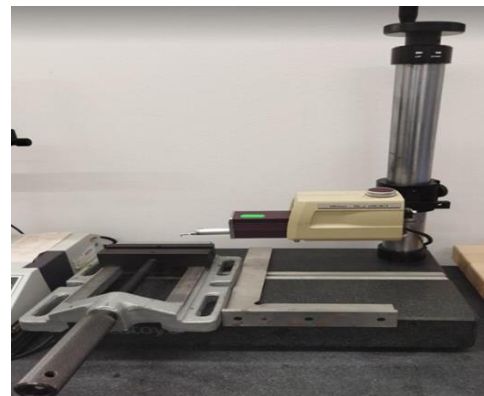


Fig. 5a: 2D/3D Surface roughness instruments:
Mitutoyo SJ-210

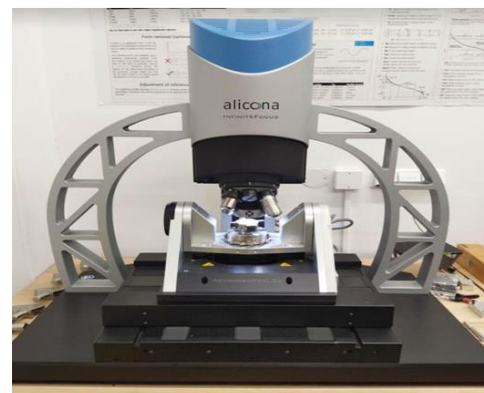


Fig. 5b: 2D/3D Surface roughness instruments:
Alicona InfiniteFocus 5G

3 RESULTS AND DISCUSSION

3.1 Measurement of 2D surface roughness

In this section, the results of the 2D surface roughness Ra and Rz are presented. Figures 6 and 7, which correspond to the data shown in Tables 3 and 4, respectively, demonstrate these roughness levels as averages for the two methods of tumbling.

The roughness values Ra showed large differences between the vibratory and centrifugal tumbling, as shown in Figure 6 as well as in Table 3 and Table 4. A comparison between sample 2 and sample 12 showed that the roughness Ra of the centrifugal tumbling was reduced many times over by tumbling with a ceramic medium compared to the initial value of the as-built sample, namely by 72% (from 12.12 µm to 3.3 µm), while it decreased by only 10% (from 12.12 µm to 10.9 µm) in the case of the vibratory tumbling. The values of the roughness Ra increased for samples 3,4 and 13,14 where they were tumbled in plastic and porcelain media respectively compared to the value of the roughness Ra in samples 2 and 12 with ceramic medium, it was discovered that the roughness Ra for centrifugal tumbling sharply decreased with increasing tumbling duration and mediums, the value of the roughness Ra in Sample 10 which was tumbled in every medium for 120 minute showed a decreased by 97% (from 12.12µm to 0.32µm), these results illustrate the effectiveness of centrifugal method to achieve the required roughness, while for the vibratory method there was only a slight effect with a small decrease with increasing of tumbling time, the lowest value of roughness Ra in the vibratory tumbling method recorded in sample 20 where it decreased only by 40% (from 12.12 2 µm to 7.39 µm) these values are insufficient to improve the surface texture of the samples. With these results, the vibratory method proved ineffective in achieving the required roughness of 2 µm.

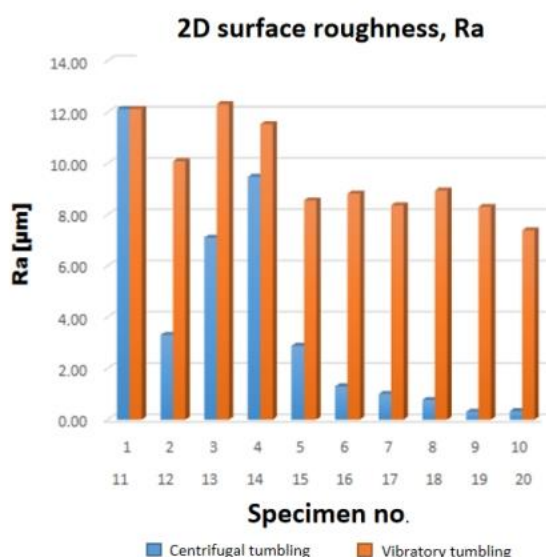


Fig. 6: 2D surface roughness Ra results grouped after centrifugal and vibratory tumbling.

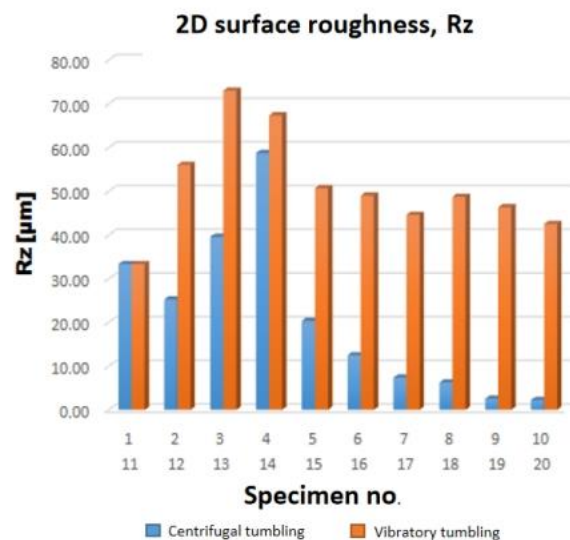


Fig. 7: 2D surface roughness Rz results grouped after centrifugal and vibratory tumbling.

The measurement of the roughness Rz confirmed the great differences between the two methods of centrifugal and vibratory tumbling, which are well explained in Figure 7 and, as it were, in Tables 3 and 4. Related to the initial value of the roughness Rz for the as-built sample, a comparison between Sample 3 and Sample 13 showed that when tumbling with plastic medium, the roughness Rz increased for both methods: it increased by 118% (from 33.35 µm to 73.05 µm) for vibratory tumbling and only by 18% (from 33.35 µm to 39.58 µm) for centrifugal tumbling. Remarkably, the roughness values of samples 4 and 14 Just like plastic medium, even porcelain in samples caused a several-fold increase in the roughness Rz. With increasing tumbling time and mediums of tumbling in the centrifugal method, there was a sharp decrease for the other samples; the minimum value of the roughness Rz was recorded for sample 10, which was reduced by 93% (from 33.35 µm to 7.39 µm). These results confirmed the effectiveness of the centrifugal method, but in the vibratory method, the opposite effect was observed; for all samples of the vibratory method, there was an increase in the roughness Rz in comparison to the as-built sample. With these results, the vibratory method proved to be undesirable.

Through the measurements of the roughness Ra and Rz, it was shown that centrifugal tumbling is more effective than vibratory tumbling. This is due to the enormous magnitude of centrifugal force in high-energy systems with the addition of the compounds, which leads to deleting the roughness in the printed samples very effectively. It is possible to efficiently prevent collisions and the resultant damage to the surfaces of the components, which makes it a safer choice. Contrarily, vibratory tumbling gives a lower radius and a smoother surface in contrast to centrifugal tumbling, making it more efficient for the finalization operation. In addition, ceramic tumbling yields more precise two-dimensional measurements than porcelain and plastic measuring techniques. Thus, ceramic medium is the best for heavy cutting and hard metal, and porcelain tumbling media is a kind of ceramic medium that has non-abrasive properties. It is used for the purposes of polishing and burnishing.

Tab. 3: 2D surface roughness results after centrifugal tumbling

Sample No.	Ra [μm]	Rz [μm]
1	12.12	33.35
2	3.30	25.25
3	7.10	39.58
4	9.48	58.76
5	2.88	20.36
6	1.29	12.50
7	1.00	7.8
8	0.76	6.24
9	0.30	2.54
10	0.32	2.24

Tab. 4: 2D surface roughness results after vibratory tumbling

Sample No.	Ra [μm]	Rz [μm]
11	12.12	33.35
12	10.09	56.06
13	12.31	73.05
14	11.53	67.36
15	8.55	50.70
16	8.82	49.00
17	8.37	44.62
18	8.94	48.74
19	8.30	46.36
20	7.39	42.54

3.2 Measurements of 3D surface structure roughness

The macro-scale images demonstrate the 3D surface roughness structure of the samples. Figures 8 and 9 show the difference in 3D structure roughness between the two methods of tumbling.

A superior surface finishing was seen in the 3D images for the centrifugal tumbling. Additionally, the ceramic medium in sample 2 exhibited a better level of roughness compared to samples 3 and 4, which were tumbled in plastic and porcelain, respectively. There was no significant change in microstructure for vibratory tumbling, and these microstructure images were consistent with 2D roughness assessments.

The first comparison was done between samples 2 and 12, after both were tumbled in ceramic media for 60 minutes. There were significant changes in surface roughness, with sample 12 having a substantially coarser surface texture after vibratory tumbling but being smooth after centrifugal tumbling. This preliminary 3D surface comparison supported the findings of the 2D surface comparison, which revealed that centrifugal tumbling was more successful than vibratory tumbling.

It was discovered that as the number of tumbling mediums increased, the surface structure improved after centrifugal tumbling and remained almost unchanged after vibratory tumbling. This observation was observed in a subsequent examination of samples 5 and 15, which were tumbled for 60 minutes in each medium. The distinction between the two forms of tumbling may be seen. Sample 5 in particular

revealed a smoothing of the surface, but sample 15's structure remained rough.

Further analysis was conducted on samples 10 and 20, which were subjected to ceramic, plastic, and porcelain mediums for a duration of 120 minutes. The study proved the inefficacy of vibratory tumbling, as it observed little alteration in the surface structure of sample 20. On the contrary, the impact of centrifugal tumbling on the surface structure of sample 10 was clearly evident. It may be inferred that increasing the duration of tumbling in the centrifugal approach leads to improved surface texture and reduced surface roughness. The comparisons of 3D surface structures validated the prior findings of 2D surfaces, indicating that centrifugal tumbling outperforms vibratory tumbling.

4 CONCLUSIONS

To sum up, this article blended two separate abrasive surface tumbling methods to give an efficient approach for treating the surfaces of AlSi10Mg powder in three different mediums for predetermined periods of tumbling. This was done in the context of printing materials with reducing spending.

Based on the results of the applied 2D and 3D measurement methods, it was discovered that centrifugal tumbling greatly improved the roughness metrics Ra and Rz for each of the samples. These results proved that the centrifugal method was more effective compared to vibratory tumbling, which was ineffective, and its application is limited to unifying the surface structure and removing supports and burrs formed during 3D printing. In addition, when finishing by tumbling was applied, it was found that the medium of tumbling and then the duration of tumbling were the major contributors to the quality of the surface roughness. It was noticed from the data obtained that the longer the sample was tumbled, the lower the roughness values Ra and Rz were found.

The centrifugal method was used on samples 9 and 10, which had a roughness of $\text{Ra} = 0.30 \mu\text{m}$. This was the lowest average Ra roughness value of all the samples examined. Samples 6, 7, and 8 tumbling methods also met the specified roughness value $\text{Ra} = 2 \mu\text{m}$. A more extensive assessment of each tumbling phase, extension to other tumbling media, and a more detailed analysis of the tumbling technique of sample 3 are all advised for a more precise interpretation of the results, which reached $\text{Ra} = 3.30 \mu\text{m}$ after 60 minutes of tumbling in the ceramic medium.

The findings of this study allow us to reach the conclusion that centrifugal tumbling is capable of producing the necessary level of roughness in a shorter amount of time, which in return helps to lower the cost of surface finishing.

5 FUTURE WORK

This work was to determine the comparison between two methods of tumbling and conclude the effectiveness of centrifugal tumbling for better surface finishing. However, this work needs to study the position of the printer samples and the scanning strategy. It is mandatory to study the effect of tumbling on the recycled AlSi10Mg powder. It is also mandatory to find the perfect time of tumbling because the medium of tumbling gives different surface roughness. According to these results, it is mandatory to study the effect of tumbling on the microhardness, surface wettability, and chemical composition behavior of tumbled samples.

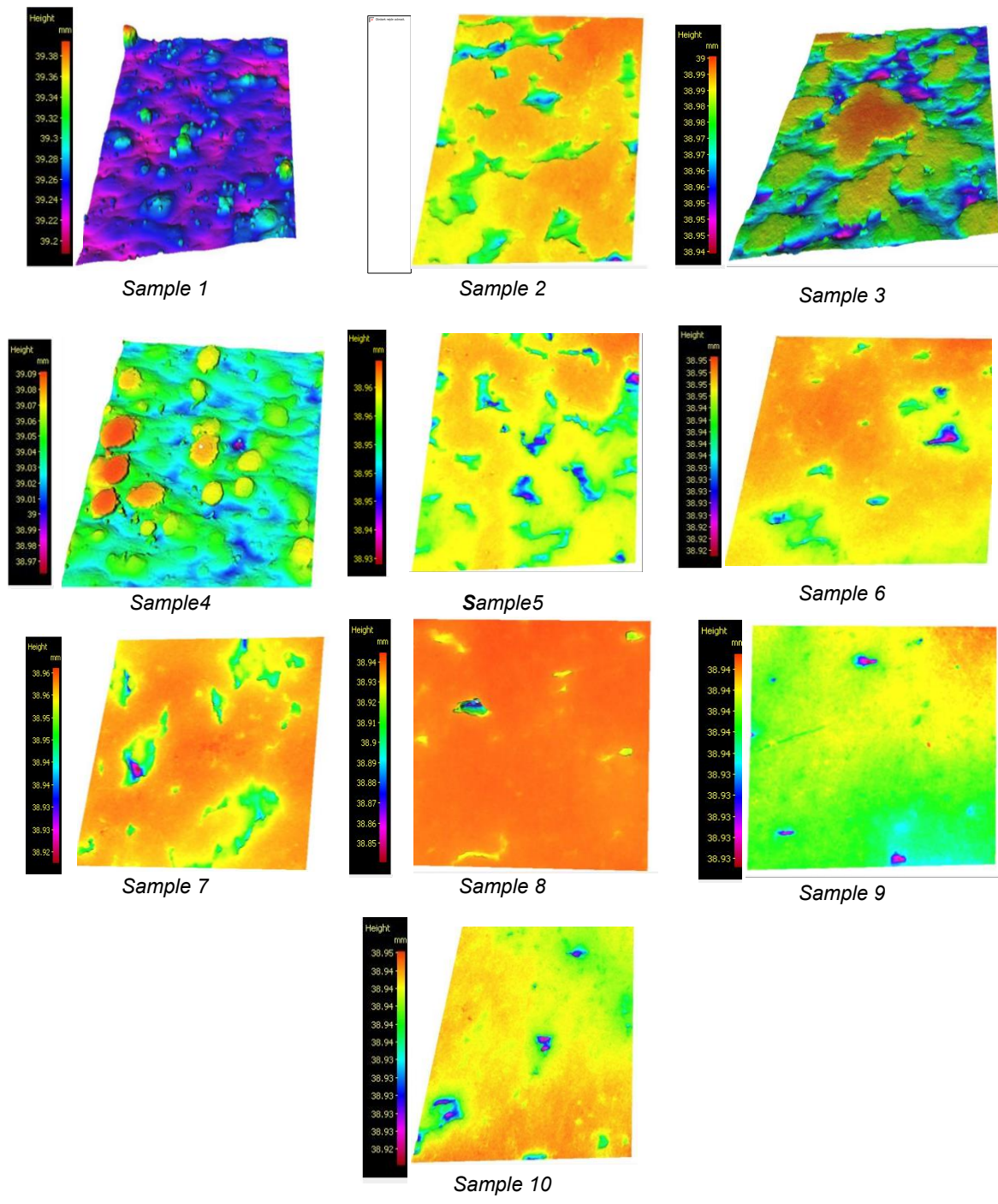


Fig. 8: 3D surface roughness with centrifugal tumbling

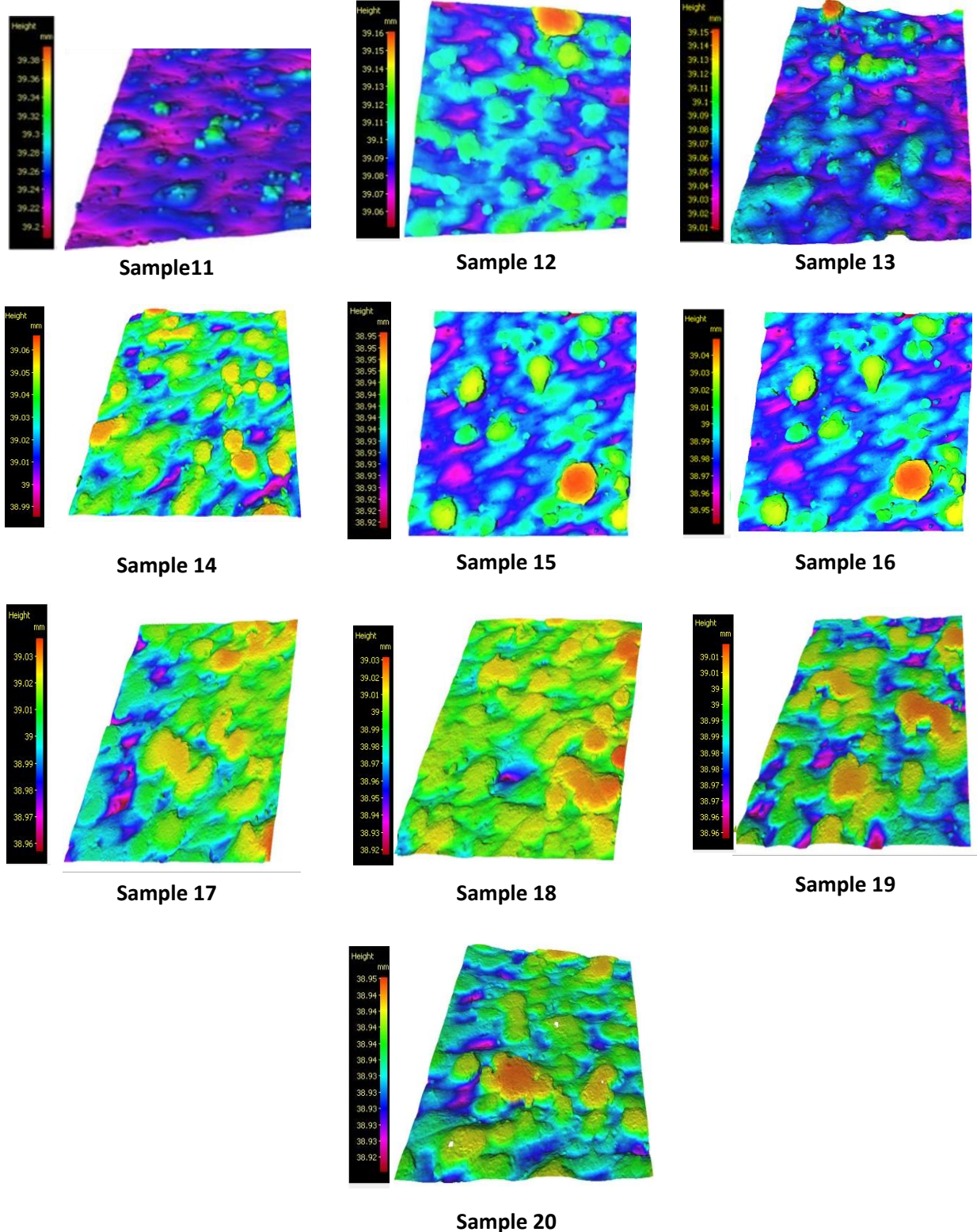


Fig. 9: 3D surface roughness with vibratory tumbling

6 ACKNOWLEDGMENTS

This article was co-funded by the European Union under the REFRESH – Research Excellence For Region Sustainability and High-tech Industries project number CZ.10.03.01/00/22_003/0000048 via the Operational Programme Just Transition. The article has been done in connection with the project Students Grant Competition SP2023/088 „Specific Research of Modern Manufacturing Technologies for Sustainable Economy “financed by the Ministry of Education, Youth and Sports and Faculty of Mechanical Engineering VŠB-TUO.

7 REFERENCES

- [Xiao 2018] Xiao, Z.; Yang, Y.; Xiao, R.; Bai, Y.; Song, C.; Wang, D. 2018. Evaluation of topology-optimized lattice structures manufactured via selective laser melting. *materials & design*, 2018, 143. <https://doi.org/10.1016/j.matdes.2018.01.023>
- [Marsalek 2020] Marsalek, P.; Sotola, M.; Rybansky, D.; Repa, V.; Halama, R.; Fusek, M.; Prokop, J. 2020. Modeling and Testing of Flexible Structures with Selected Planar Patterns Used in Biomedical Applications. *Materials*, 14(1), 140. <https://doi.org/10.3390/ma14010140>
- [Pagac 2018] Pagac, M.; Hajnys, J.; Petru, J.; Zlamal, T. 2018. Comparison of Hardness of Surface 316L Stainless Steel Made by Additive Technology and Cold Rolling. *Materials Science Forum*, 919, 84-91. <https://doi.org/10.4028/www.scientific.net/MSF.919.84>
- [Liverani 2017] Liverani, E.; Toschi, S.; Ceschini, I.; Fortunato, A. 2017. Effect of selective laser melting (SLM) process parameters
- [Hlinka 2020] Hlinka, J.; Kraus, M.; Hajnys, J.; Pagac, M.; Petru, J.; Brytan, Z.; Tanski, T. 2020. Complex Corrosion Properties of AISI 316L Steel Prepared by 3D Printing Technology for Possible Implant Applications. *Materials*, 13(7), 1527. <https://doi.org/10.3390/ma13071527>
- [Chen 2018] Chen, Z.; Wu, X.; Tomus, D.; Davies, C. 2018. surface roughness of selective laser melted ti-6al-4v alloy components. *Additive Manufacturing*, 21, 91–103. <https://doi.org/10.1016/j.addma.2018.02.009>
- [Mohammadian 2018] Mohammadian, N.; Turenne, S.; Brailovski, V. 2018. Surface finish control of additively-manufactured Inconel 625 components using combined chemical-abrasive flow polishing. *Journal of Materials Processing Technology*, 252, 728–738. <https://doi.org/10.1016/j.jmatprotec.2017.10.020>
- [Strano 2013] Strano, G.; Hao, L.; Everson, R.; Evans, K. 2013. Surface roughness analysis, modelling and prediction in selective laser melting, *Journal of Materials Processing Technology*, 213, 589–597. <https://doi.org/10.1016/j.jmatprotec.2012.11.011>
- [Cep 2014] Cep R.; Janasek A.; Petru J.; Sadilek M.; Mohyla P.; Valicek J.; Harnicarova M.; Czan A. Surface Roughness after Machining and Influence of Feed Rate on Process, *Key Engineering Materials: Precision Machining VII*, Vol. 581. <https://doi.org/10.4028/www.scientific.net/KEM.581.341>
- [Wang 2016] Wang, D.; Liu, Y.; Yang, Y.; Xiao, D. 2016, Theoretical and experimental study on surface roughness of 316L stainless steel metal parts obtained through selective laser melting. *Rapid Prototyping Journal*, 22, 706–716. <https://doi.org/10.1108/RPJ-06-2015-0078>
- [Leary 2017] Leary, M. 2019. Surface Roughness Optimisation for Selective Laser Melting (SLM): Accommodating Relevant and Irrelevant Surfaces; RMIT University, Centre for Additive Manufacturing: Melbourne, VIC, Australia; pp. 99–118. <https://doi.org/10.1016/B978-0-08-100433-3.00004-X>
- [Vayssette 2018] Vayssette, B.; Saintier, N.; Brugger, C.; Elmay, M.; Pessard, E. 2018. Surface roughness of Ti-6Al-4V parts obtained by SLM and EBM: Effect on the High Cycle Fatigue life on microstructure and mechanical properties of 316L austenitic stainless steel. *Journal of Materials Processing Technology*, 249, 255–263. <https://doi.org/10.1016/j.jmatprotec.2017.05.042>
- [Yakout 2019] Yakout, M.; Elbestawi, M.; Veldhuis, S. 2019. Density and mechanical properties in selective laser melting of Invar 36 and stainless steel 316L. *Journal of Materials Processing Technology*, 266, 397–420. <https://doi.org/10.1016/j.jmatprotec.2018.11.006>
- [Procedia Engineering, 2018] Procedia Engineering, 213, 89–97. <https://doi.org/10.1016/j.proeng.2018.02.010>
- [Townsend 2016] Townsend, A.; Senin, N.; Blunt, L.; Leach, R.; Taylor, J. 2016. Surface texture metrology for metal additive manufacturing: A review. *Precision Engineering*, 46, 34–47. <https://doi.org/10.1016/j.precisioneng.2016.06.001>
- [Kaynak 2018] kaynak, y.; kitay, o. 2018. Porosity, Surface Quality, Microhardness and Microstructure of Selective Laser Melted 316L Stainless Steel Resulting from Finish Machining. *Manufacturing and Materials Processing*, 2, 36. <https://doi.org/10.3390/jmmp2020036>
- [Hajnys 2020] Hajnys, J.; Pagac, M.; Mesicek, J.; Petru, J.; Spalek, F. 2020. Research of 316L Metallic Powder for Use in SLM 3D Printing. *Advances in Materials Science*. 2020, 20, 5–15. <https://doi.org/10.2478/adms-2020-0001>
- [Kozior 2020] Kozior, T.; Bochnia, J. 2020. The Influence of Printing Orientation on Surface Texture Parameters in Powder Bed Fusion Technology with 316L Steel. *Micromachines*, 11, 639. <https://doi.org/10.3390/mi11070639>
- [Cillikova 2022] Cillikova M.; Micetova A.; Cep R.; Jackova M.; Minarik P.; Neslusan M.; Kouril K. Analysis of Surface State after Turning of High Tempered Bearing Steel, vol 15, No. 5. <https://doi.org/10.3390/ma15051718>.
- [Bin 2018] Bin, L.; Zezhou, K.; Zhonghua, L.; Jianbin, T.; Peikang, B.; Baoqiang, L. 2018. Performance Consistency of AlSi10Mg Alloy Manufactured by Simulating Multi Laser BeamSelective Laser Melting (SLM): Microstructures and Mechanical Properties, *Materials*, 11, 2–18. <https://doi.org/10.3390/ma11122354>
- [Mesicek 2022] Mesicek, J.; Cegan, T.; Ma, Q.-P.; Halama, R.; Skotnicova, K.; Hajnys, J.; Jurica, J.; Krpec, P.; Pagac, M. 2022. Effect of Artificial Aging on the Strength, Hardness, and Residual Stress of SLM AlSi10Mg Parts Prepared from the Recycled Powder. *Materials Science and Engineering*, 855, 1–18. <https://doi.org/10.1016/j.msea.2022.143900>